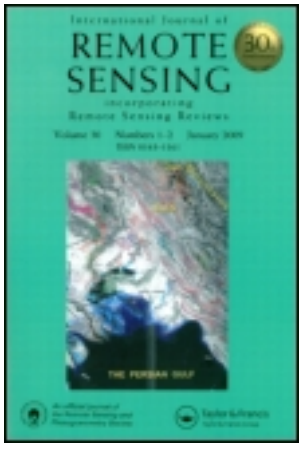

International Journal of Remote Sensing
Publication details, including instructions for authors and subscription information:
http://www.tandfonline.com/loi/tres20

Estimation of the North-South Transect of Eastern China forest biomass using remote sensing and forest inventory data

Yanhua Gao [a b], Xinxin Liu [c], Chengcheng Min [a d], Honglin He [a], Guirui Yu [a], Min Liu [a], Xudong Zhu [a] & Qiao Wang [b]

[a] Key Laboratory of Ecosystem Network Observation and Modelling, Institute of Geographic Sciences and Natural Resources Research,CAS , Beijing , 100101 , China

[b] Satellite Environment Centre, Ministry of Environment Protection , Beijing , 100094 , China

[c] Jinan City Planning Consultation Service Centre , Jinan , 250014 , China

[d] Faculty of Resources and Environmental Science, Hubei University , Wuhan , 430062 , China

Published online: 08 May 2013.

To cite this article: Yanhua Gao , Xinxin Liu , Chengcheng Min , Honglin He , Guirui Yu , Min Liu , Xudong Zhu & Qiao Wang (2013) Estimation of the North-South Transect of Eastern China forest biomass using remote sensing and forest inventory data, International Journal of Remote Sensing, 34:15, 5598-5610, DOI: 10.1080/01431161.2013.794985

To link to this article: http://dx.doi.org/10.1080/01431161.2013.794985

International Journal of Remote Sensing, 2013
Vol. 34, No. 15, 5598–5610, http://dx.doi.org/10.1080/01431161.2013.794985

Estimation of the North–South Transect of Eastern China forest biomass using remote sensing and forest inventory data

Yanhua Gao[a,b], Xinxin Liu[c], Chengcheng Min[a,d], Honglin He[a]*, Guirui Yu[a], Min Liu[a], Xudong Zhu[a], and Qiao Wang[b]

[a]*Key Laboratory of Ecosystem Network Observation and Modelling, Institute of Geographic Sciences and Natural Resources Research, CAS, Beijing 100101, China;* [b]*Satellite Environment Centre, Ministry of Environment Protection, Beijing 100094, China;* [c]*Jinan City Planning Consultation Service Centre, Jinan 250014, China;* [d]*Faculty of Resources and Environmental Science, Hubei University, Wuhan 430062, China*

(*Received 16 August 2011; accepted 20 January 2013*)

The assessment of forest biomass is required for the estimation of carbon sinks and a myriad other ecological and environmental factors. In this article, we combined satellite data (Thematic Mapper (TM) and Moderate Resolution Imaging Spectrometer (MODIS)), forest inventory data, and meteorological data to estimate forest biomass across the North–South Transect of Eastern China (NSTEC). We estimate that the total regional forest biomass was 2.306×10^9 Megagrams (Mg) in 2007, with a mean coniferous forest biomass density of 132.78 Mg ha^{-1} and a mean broadleaved forest biomass density of 142.32 Mg ha^{-1}. The mean biomass density of the entire NSTEC was 129 Mg ha^{-1}. Furthermore, we analysed the spatial distribution pattern of the forest biomass and the distribution of biomass along the latitudinal and longitudinal gradients. The biomass was higher in the south and east and lower in the north and west of the transect. In the northern part of the NSTEC, the forest biomass was positively correlated with longitude. However, in the southern part of the transect, the forest biomass was negatively correlated with latitude but positively correlated with longitude. The biomass had an increasing trend with increases in precipitation and temperature. The results of the study can provide useful information for future studies, including quantifying the regional carbon budget.

1. Introduction

As the principal component of the terrestrial ecosystem, the forest ecosystem represents one of the major carbon pools. As climate change accelerates, the strong carbon sink capacity of forest ecosystems increasingly attracts the interest of international communities. Except for some small areas that have been carefully studied, estimates of carbon sink capacity are subject to a high degree of uncertainty. One useful way to proceed is to estimate biomass changes in land cover (Lu 2006). A number of studies have provided useful approaches for estimating forest biomass, and remote-sensing technology has become the most effective method due to its convenience of data acquisition, its synoptic view over large areas, and its greatly increased efficiency and usefulness in comparison with the limited conventional methods. Numerous studies have estimated forest biomass

*Corresponding author. Email: hehl@igsnrr.ac.cn

at different scales using remote-sensing data (Roy and Ravan 1996; Barbosa et al. 1999; Nelson et al. 2000; Wylie et al. 2002; Dong et al. 2003; Foody 2003; Thenkabail 2004; Zheng et al. 2004; Lu 2005; Muukkonen and Heiskanen 2007). Because fine-spatial resolution remote-sensing data (IKONOS, QuickBird) match well with ground measurements in terms of spatial resolution, these can be combined to establish a biomass estimate model. Coarse spatial-resolution remote-sensing data (Advanced Very High Resolution Radiometer (AVHRR), Système Pour l'Observation de la Terre (SPOT) VEGETATION, Moderate Resolution Imaging Spectrometer (MODIS)) have been useful in regional- or even global-scale forest biomass estimation due to their wide image coverage and frequency of data acquisition (Muukkonen and Heiskanen 2007). Medium-resolution satellite data (TM, Advanced Spaceborne Thermal Emission and Reflection Radiometer (ASTER)) can be used as an intermediate step in linking plot-level field measurements with coarse-resolution remote-sensing data (Tomppo et al. 2002).

In this study, a large body of forest biomass inventory data and 30 m resolution TM data were combined to build forest biomass estimation models. By means of spectral calibration between TM and MODIS sensors, the models were utilized to estimate the regional forest biomass of the North–South Transect of Eastern China (NSTEC) with MODIS data. We analysed the relationship between forest biomass and vegetation indices, geo-factors, and meteorological factors, and we demonstrate the spatial distribution pattern of forest biomass within the context of the NSTEC.

2. Materials and methods

We modelled the NSTEC biomass using remote sensing and forest investigation data using two sets of remote-sensing data, one with a smaller pixel size (TM, 30 m) and the other with a larger pixel size (MODIS, 250 m) for model parameterization and application at the regional scale. Detailed steps included the following: (1) developing the forest biomass model within a limited portion of the region using TM and forest inventory data; (2) conducting internal spectral calibrations between TM and MODIS data due to differences in spatial and spectral resolutions between the two sensors such that the TM-based model can be applied to the entire region of NSTEC using MODIS data; and (3) validating the model and analysing the distribution of forest biomass in the NSTEC.

2.1. Study area

The NSTEC is a concentrated forest distribution area in China and spans a wide range of environmental conditions including temperature, precipitation, and topography. The NSTEC extends from Hainan Island to the northern border of China, ranging between longitudes 108–118° E for latitudes below 40° N and longitudes 118–128° E for latitudes equal to or greater than 40° N, and covers about 1/3 of the territory of China (Figure 1). The northern part extends from the north of the Da Hinggan Mountains eastward to Changbaishan through Xiao Hinggan Mountains (118° E, 55° N to 128° E, 40° N). The southern part extends from the North China Plain through the Yangtze–Huai Plain, the Chiang-nan Hilly Region, and the Nanling Mountains to Hainan Island (108° E, 40° N to 118° E, 17.5° N). The straight-line distance from south to north is over 3500 km. There are large heat and water-heat group gradients in the NSTEC (Peng et al. 2002). The annual mean temperature in the transect ranges from 24°C in Hainan Province to 0–4°C in Heilongjiang Province, and annual precipitation values range accordingly. The Yangtze River can be regarded as the natural rainfall isoline of 1000 mm; to the south, rainfall

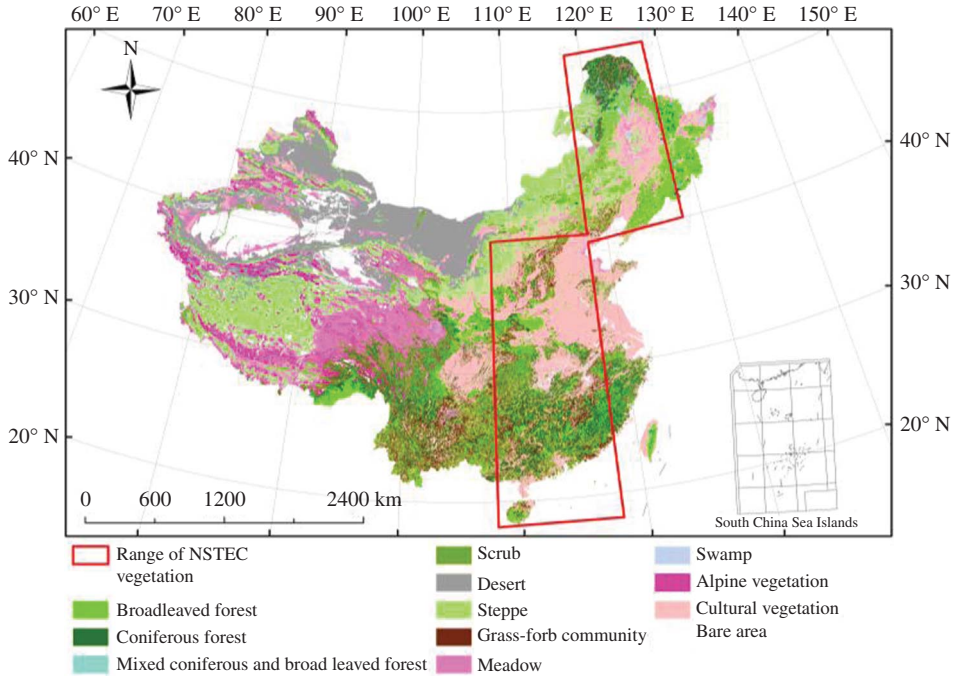

Figure 1. Geographic range of the North–South Transect of Eastern China (NSTEC) and its land-cover types.

increases gradually to 1600 mm in Fujian, Hunan, Jiangxi, and Hubei provinces, and to the north it decreases to 600 mm in Northeast China (Zhou and Zhang 2008). The main types of vegetation from south to north range from tropical evergreen forest, mixed tropical evergreen and deciduous forest, subtropical evergreen forest, mixed subtropical evergreen and deciduous forest, subtropical coniferous, warm deciduous broadleaved forest, warm needle, mixed warm broadleaved, and coniferous forest, subalpine deciduous coniferous and warm alpine evergreen coniferous, to alpine coniferous (Wu 1980).

2.2. Data and processing

The field biomass data were derived from the dissertation of Luo (Luo 1996), which includes forest biomass data from the 1980s and 1990s throughout China. This data set includes biomass, net primary productivity (NPP), leaf area index (LAI), and atmospheric data from 1266 plots. To match the time of the field biomass data, TM images dating from July to September in the 1980s/1990s and derived from the Global Land Survey (GLS) 1990 data set were acquired to build the biomass model. Furthermore, the 2006–2007 Landsat TM data and MODIS 250 m data (MOD09Q1) dating from July to September were collected to conduct spectral calibrations between them. The study area is covered by 200 scenes of TM images, and by 13 scenes of MODIS images. To minimize cloud contamination and atmospheric effects, we collected TM imagery with as little cloud cover as possible. Atmospheric correction of Landsat data was performed using the FLAASH module of ENVI software which is manufactured by ITT Visual Information Solutions (ITT VIS, Boulder, CO, USA), and geometric rectification and mosaicking were performed.

NASA provides a range of MODIS products pre-processed with standard correction algorithms. MODIS 09 daily data were corrected for the effects of gaseous and aerosol scattering and absorption, as well as for adjacency effects caused by variation in land cover, bidirectional reflectance distribution function (BRDF) and atmosphere coupling effects, and contamination by thin cirrus (Vermote and Vermeulen 1999). In particular, each MOD09Q1 data granule (MODIS/Terra Surface Reflectance 8 Day L3 Global 250 m SIN Grid) offers a composite of the previous eight daily surface reflectance products with the best observations for each pixel in the two MODIS bands at 250 m (red and near-infrared). The goal is to obtain single cloud-free images with minimal atmospheric and sun surface–sensor angular effects representative of the 8 day period (Rossi et al. 2010). MOD09Q1 images dating from July to September have been collected for the years 2006–2007 and re-projected using the MODIS Reprojection Tool (MRT). All data were projected to the Albers Conical Equal Area.

The other spatial data applied in this article include 1 km resolution digital elevation models (DEMs) from the National Fundamental Geographic Information System (NFGIS) and a 1:1,000,000 vegetation map of China derived from the Vegetation Atlas of China (Hou 2001). Another important data source was the 2001–2007 average precipitation and temperature data from 752 atmospheric observation sites, which were interpolated to individual 1 km pixels using ANUSPLINE (Hutchinson 2001). Average precipitation and temperature data were interpolated using thin-plate smoothing splines based on the topography of the transect.

2.3. Model development

Two hundred scenes of TM images in the 1980s/1990s for the study area were acquired to calculate various vegetation indices, which were used to assess the status of and monitor the evolution of the terrestrial biosphere. These vegetation indices have varying sensitivity to atmospheric or soil conditions. In this article, we chose four indices (NDVI, RVI, SAVI, and MSAVI) to perform multiple linear regression analysis, and those with good capability to retrieve forest biomass from TM were determined based on the Statistical Program for Social Sciences (SPSS). The relative data on surface reflectivity, which are manifested in the image digital numbers (DN), were converted to an absolute form, reflectance, prior to the calculation of vegetation indices (Foody, Boyd, and Cutler 2003). Four vegetation indices were selected for the statistical modelling.

(1) Normalized difference vegetation index (NDVI): $\mathrm{NDVI} = {\rho_{\mathrm{NIR}} - \rho_{\mathrm{R}}}/{\rho_{\mathrm{NIR}} + \rho_{\mathrm{R}}}$.
(2) Ratio vegetation index (RVI): $\mathrm{RVI} = {\rho_{\mathrm{NIR}}}/{\rho_{\mathrm{R}}}$.
(3) Soil-adjusted vegetation index (SAVI) (Huete 1988): $\mathrm{SAVI} = ({\rho_{\mathrm{NIR}} - \rho_{\mathrm{R}}}/{\rho_{\mathrm{NIR}} + \rho_{\mathrm{R}} + L})(1 + L)$, where L is the soil brightness correction factor; $L = 0.5$ works well in most situations and is the default value (Qi et al. 1994).
(4) Modified soil-adjusted vegetation index (MSAVI):

$$\mathrm{MSAVI} = \frac{\left[(2\rho_{\mathrm{NIR}} + 1) - \sqrt{(2\rho_{\mathrm{NIR}} + 1)^2 - 8\,(\rho_{\mathrm{NIR}} - \rho_{\mathrm{R}})}\right]}{2}.$$

In the above equation, ρ_{R} and ρ_{NIR} are the bands reflectance of red (R) and near infrared (NIR), respectively.

Table 1. Statistical models used for biomass estimation.

Model	Equation	r
$\text{Model}_{\text{ove}}$	$Y = 0.129 \times v_{\text{precip}} - 0.029 \times u_{\text{alt}} + 3.418 \times g_{\text{temp}} + 5.151 \times (\text{RVI}) + 41.963$	0.626
$\text{Model}_{\text{con}}$	$Y = 0.088 \times v_{\text{precip}} - 0.028 \times u_{\text{alt}} + 3.059 \times g_{\text{temp}} + 3.272 \times (\text{RVI}) + 68.543$	0.572
$\text{Model}_{\text{bro}}$	$Y = 0.152 \times v_{\text{precip}} - 0.039 \times u_{\text{alt}} + 3.304 \times g_{\text{temp}} + 55.097 \times (\text{NDVI}) + 36.541$	0.722

Notes: $\text{Model}_{\text{ove}}$ is the overall forest biomass estimation model for all forests within the NSTEC; this model did not distinguish forest types. $\text{Model}_{\text{con}}$ and $\text{Model}_{\text{bro}}$ are biomass estimation models for coniferous forest and broadleaved forest, respectively. Y represents biomass density (Mg ha^{-1}), v_{precip} represents average annual precipitation (mm), u_{alt} represents altitude (m), and g_{temp} represents average annual temperature (°C). RVI, ratio vegetation index; NDVI, normalized difference vegetation index.

Biomass estimation models were established through multiple linear regression analysis (see Table 1). The optimal independent variables were determined through stepwise regressions from four vegetation indices, reflectance in bands 3 and 4, average annual precipitation, average annual temperature, and DEM. Stepwise linear regression is a semi-automated process of building a model by successively adding or removing variables based solely on the t-statistics of their estimated coefficients. Using all the field biomass data, we built the overall forest biomass estimation model ($\text{Model}_{\text{ove}}$) for all forests within the NSTEC; this model did not distinguish among forest types. Therefore, we also built two biomass estimation models, one for coniferous forest ($\text{Model}_{\text{con}}$) and the other for broadleaved forest ($\text{Model}_{\text{bro}}$), by splitting the field biomass into two groups.

2.4. Spectral calibrations between two sensors

The biomass estimation model driven by TM is limited when applied to biomass estimations of large areas, because of economic constraints. To provide a readily available and low-cost method for the biomass estimation of a large area, model transformation was performed to apply TM-based models to the NSTEC with MODIS data.

The linear regression equations, expressed as $Y = aX + b$, were established to transform the spectral reflectance of MODIS bands 1 and 2 into those of TM bands 3 and 4, respectively (Hame et al. 1997; Muukkonen and Heiskanen 2007). In this equation, Y represents the spectral reflectance of TM and X represents the spectral reflectance of MODIS. The constant parameters, a and b, were calculated based on Equations (1) and (2), respectively:

$$a = \frac{\sigma(y)}{\sigma(x)}, \tag{1}$$

$$b = \bar{y} - a\bar{x}. \tag{2}$$

In Equations (1) and (2), $\bar{y}$ and $\bar{x}$ are the mean values of variables y and x, and $\sigma(y)$ and $\sigma(x)$ are their standard deviations, respectively (Curran and Hay 1986).

The forest-cover map of the NSTEC was extracted from the 1:1,000,000 vegetation map and used as a mask to calculate the mean value and standard deviation of reflectance of each band. Thus, the constant parameters a and b could be calculated by Equations (1) and (2). Therefore, the linear regression models were determined as follows:

Table 2. Precision detection and statistics of the models.

Model	ME	MAE	MRE (%)	MARE (%)	p
$\text{Model}_{\text{ove}}$ (75 samples)	45.549	78.613	2.2	35.3	0.875
$\text{Model}_{\text{con}}$ (35 samples)	47.088	68.164	10.5	48.8	0.706
$\text{Model}_{\text{bro}}$ (40 samples)	−18.916	42.579	−30.7	42.1	0.905

Notes: $\text{Model}_{\text{ove}}$ is the overall forest biomass estimation model for all forests within the NSTEC. $\text{Model}_{\text{con}}$ and $\text{Model}_{\text{bro}}$ are biomass estimation models for coniferous and broadleaved forest, respectively.

$$Y_{\text{TM3}} = 0.188X_{\text{MODIS1}} + 0.018, \tag{3}$$

$$Y_{\text{TM4}} = 0.464X_{\text{MODIS2}} + 0.030. \tag{4}$$

In Equations (3) and (4), Y_{TM3} and Y_{TM4} are the spectral reflectances of TM bands 3 and 4, respectively, and X_{MODIS1} and X_{MODIS2} are the spectral reflectances of MODIS bands 1 and 2, respectively.

2.5. Model validation

An evaluation of the model's performance and an assessment of the accuracy of the estimated results are important aspects of the biomass estimation procedure. The randomly reserved data were used for the model-independent test, which was not involved in the statistical modelling; these accounted for 10% of the data (Mayer and Butler 1993). The statistical indicators listed below indicated that there was a good fit between the developed model and sample data (see Table 2).

(1) Mean error (ME): $\text{ME} = \sum_{i=1}^{n} \left(\frac{y_i - \hat{y}_i}{n} \right)$.

(2) Mean absolute error (MAE): $\text{MAE} = \sum_{i=1}^{n} \left| \frac{y_i - \hat{y}_i}{n} \right|$.

(3) Average relative error (MRE): $\text{MRE} = \frac{1}{n} \sum_{i=1}^{n} \left(\frac{y_i - \hat{y}_i}{y_i} \right) \times 100\%$.

(4) Mean absolute relative error (MARE): $\text{MARE} = \sum_{i=1}^{n} \left| \frac{y_i - \hat{y}_i}{y_i} \right| \times 100\%$.

(5) Precision of model estimation (p): $p = (1 - \frac{t_{0.05} S_{\bar{y}}}{\hat{\bar{y}}}) \times 100\%$.

In these equations, $\hat{\bar{y}}$ is the mean value of the estimation and $S_{\bar{y}}$ is the standard error of the regression.

3. Results and discussion

3.1. Distribution of forest biomass

The forest biomass within the NSTEC was estimated independently by an overall model and two categorization models. As a result, three forest biomass distribution maps were produced (see Figures 2(*a*)–(*c*)). Figure 2 shows that the forest biomass derived from the

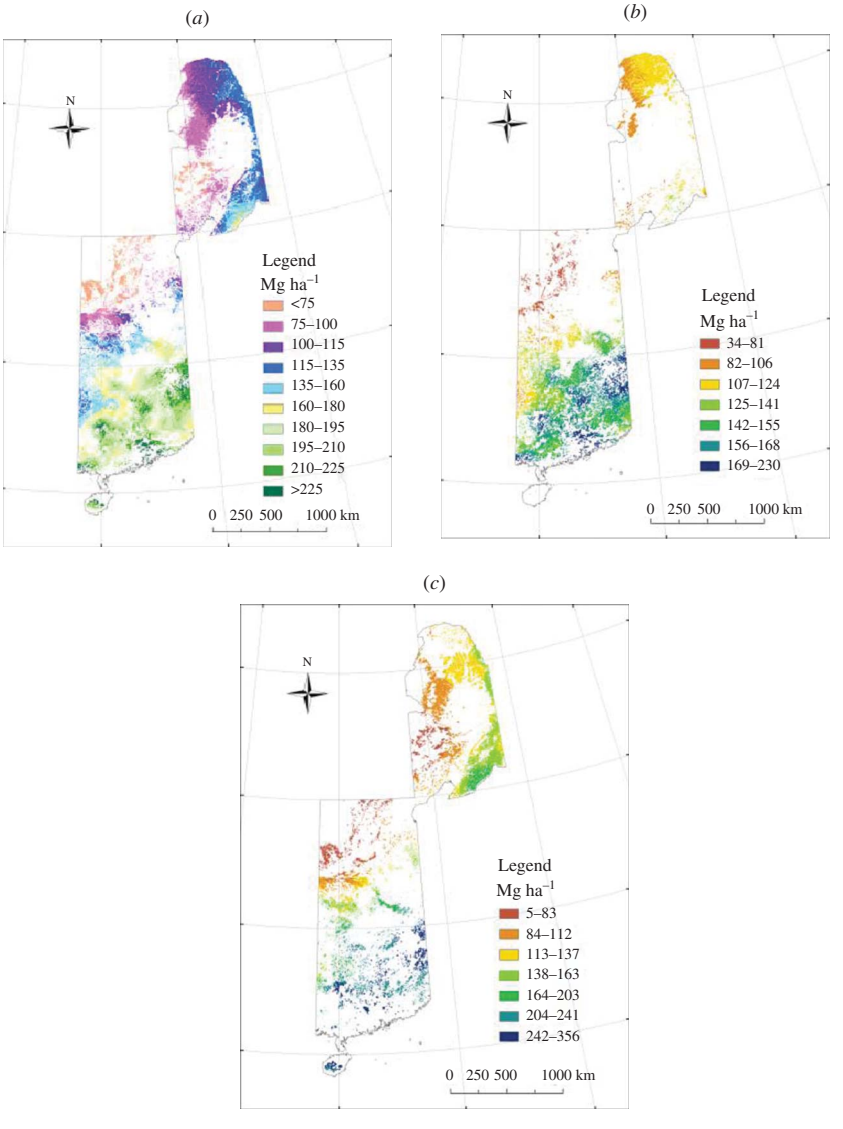

Figure 2. Spatial distribution of forest (all types) biomass estimated from stepwise regression models (*a*) $Model_{ove}$, (*b*) $Model_{con}$, and (*c*) ($Model_{bro}$).

overall model ranges from 30 Megagrams (Mg) ha^{-1} to 308 Mg ha^{-1}. Figures 3 and 4 indicate that the biomass of coniferous forest ranges from 34 Mg ha^{-1} to 240 Mg ha^{-1}, with a mean value of 132.78 Mg ha^{-1}, while broadleaved forest ranges from 4 Mg ha^{-1} to 240 Mg ha^{-1}, with a mean value of 142.32 Mg ha^{-1}. The biomass distribution trends of coniferous forest and broadleaved forest derived from the overall estimation model were essentially the same as those derived from the categorization models, both of which were higher in the south and east and lower in the north and west of the transect.

To reveal the spatial distribution pattern of the forest biomass within the context of the NSTEC, the entire transect was divided into two parts, northern and southern, by 40° N latitude. We divided the northern and southern parts into strips along the directions of

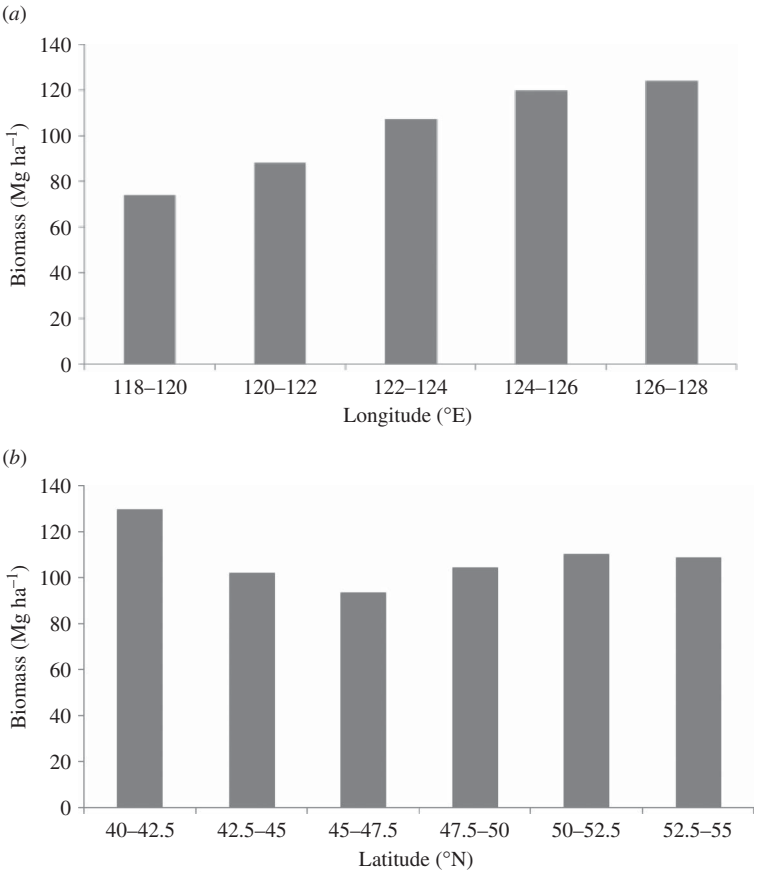

Figure 3. Allocation of average biomass per unit forest area in strips along the direction of longitude (*a*) and the direction latitude (*b*) in the northern part of the North–South Transect of Eastern China (NSTEC).

longitude and latitude, respectively, both of which are 2.5° of latitude or longitude in width. For each strip, we acquired the average biomass per unit forest area to analyse the spatial distribution of forest biomass in the entire transect.

3.1.1. Distribution of forest biomass in the northern part of the NSTEC

The northern part of the NSTEC stretched from Heilongjiang Province to Liaoning Province through Inner Mongolia and was dominated by sub-boreal and temperate alpine coniferous forest, temperate deciduous broadleaved forest, temperate deciduous woodland, and temperate coniferous forest. The forest consisted of several tree species including *Larix gmelinii*, *Quecus mongolica*, *Betula platyphylla*, *Ulmus*, *Populus*, *Quercus liaotungensis*, and *Pinus tabulaeformis*.

The northern part of the NSTEC was divided into five strips along the direction of longitude, and into six strips along the direction of latitude. The average biomass per unit forest area in strips along the direction of longitude showed forest biomass longitudinal trends, while along the direction of latitude it showed latitudinal trends.

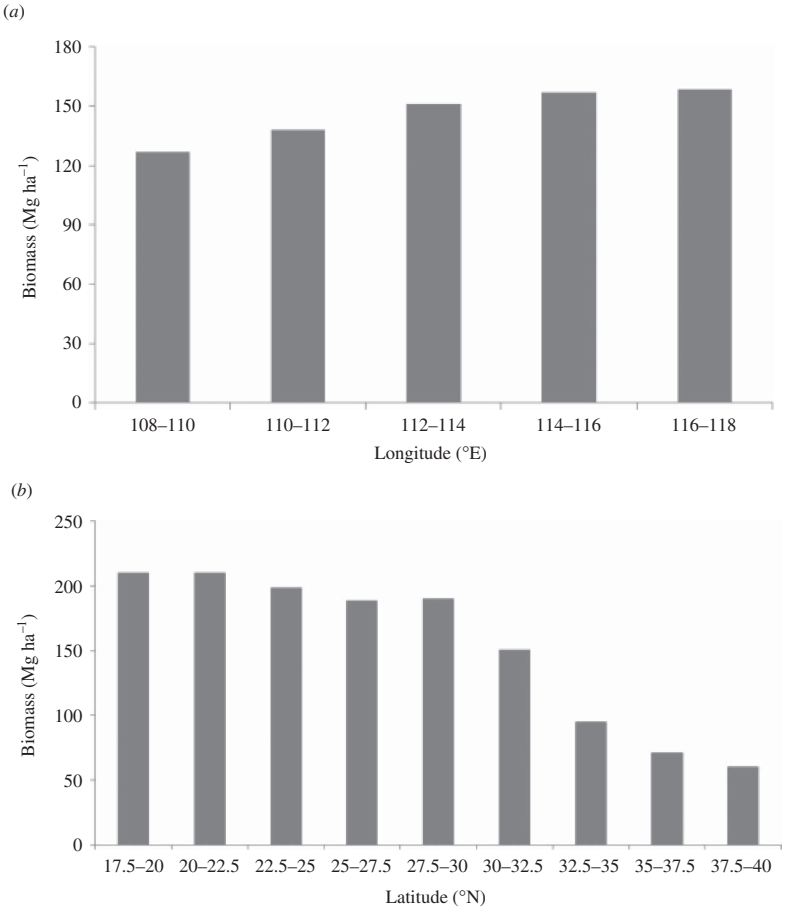

Figure 4. Allocation of average biomass per unit forest area in strips along the direction of longitude (*a*) and the direction of latitude (*b*) in the southern part of the North–South Transect of Eastern China (NSTEC).

As shown in Figure 3(*a*), the average biomass per unit forest area in strips along the direction of longitude ranged from 78 Mg ha^{-1} to 124 Mg ha^{-1}, and forest biomass generally increased with increasing longitude. Biomass was relatively high between longitudes 125° E and 132.5° E because the Hinggan Mountains and Changbai Mountains are located in this area, both having immense forested areas, high forest cover, and intact forest ecosystems.

The average biomass per unit forest area in strips along the direction of latitude ranged from 93.5 Mg ha^{-1} to 129.7 Mg ha^{-1}, a trend showing relatively small fluctuation. The level of 45° N was a turning point below which biomass decreased markedly from 129.7 Mg ha^{-1} to 93.5 Mg ha^{-1}, above which it changed little, especially above 47.5° N (see Figure 3(*b*)). Fluctuation in biomass is caused by the location of the Hinggan and Changbai Mountains. The high biomass from 40° N to 45° N is mainly due to the Changbai Mountains, with high forest cover and an intact forest ecosystem. The relatively high and steady-state biomass between 47.5° N and 55° N is contributed to by the intact forest ecosystem of the Hinggan Mountains.

3.1.2. Distribution of forest biomass in the southern part of the NSTEC

The southern part of the NSTEC crosses a broad span of latitude (23–40° N). From south to north, the forest types are subtropical coniferous forest, subtropical evergreen and deciduous broadleaved mixed forest, subtropical bamboo forest, subtropical evergreen broadleaved forest, temperate deciduous broadleaved forest, temperate coniferous forest and sub-boreal, and temperate alpine coniferous forest.

The southern part of the NSTEC was divided into five strips along the direction of longitude and nine strips along the direction of latitude. The average biomass per unit forest area in strips along the direction of longitude showed forest biomass longitudinal trends, while along the direction of latitude it showed latitudinal trends.

Figure 4(*a*) shows that the average biomass per unit forest area in strips along the direction of longitude ranged from 140 Mg ha^{-1} to 191 Mg ha^{-1}, and that forest biomass generally increased with increasing longitude. The average biomass per unit forest area in strips along the direction of latitude ranged from 60 Mg ha^{-1} to 210 Mg ha^{-1}, showing greater variation than that along the direction of longitude; the level of 30° N was a turning point below which biomass changed little, and above which biomass decreased markedly from approximately 190 Mg ha^{-1} to 60 Mg ha^{-1} (see Figure 4(*b*)). Temperature in the various heat zones is one of the main factors resulting in this distribution biomass pattern. However, high-intensity human disturbance and the development of secondary forest are also important factors in bringing about a marked reduction in biomass in the area between 30° N and 40° N. Over the whole transect, high-intensity human disturbance in this area has led to a huge discrepancy between biomass at latitudes 37.5–40.0° N and 40.0–42.5° N (Figures 3(*b*) and 4(*b*)).

3.2. Gradient distribution of biomass in regard to climatic factors

The NSTEC is characterized by complex topography and environmental conditions. Marked spatial variation in solar energy and available water and nutrients along the transect is the primary cause of the diverse distribution of terrestrial ecosystems and biomass. To clarify the extent to which climatic factors determine biomass along the gradient of climatic factors, we calculated the average biomass per unit forest area in relation to precipitation and temperature levels.

The average annual precipitation within the NSTEC varies between 211 mm and 2536 mm. We split these values into gradients of 100 mm, resulting in 15 precipitation levels, and the average biomass per unit forest area was calculated for each precipitation level (see Figure 5). As shown in the graph, biomass exhibits an overall increasing trend as precipitation increases, becoming more significant when precipitation exceeds 800 mm. Because this level of precipitation is the dividing line between the humid and sub-humid regions of China (Wu et al. 2005), we conclude that biomass is increased in the humid regions of China.

A similar method was used to determine the extent to which temperature impacts on biomass at each temperature level. The average annual temperature within the NSTEC varied between –7°C and 27°C and was divided into 17 levels with a gradient of 2°C, and the average biomass per unit forest area was calculated for each temperature level. Figure 6 shows that 11°C is a turning point below which biomass changes little, remaining at approximately 100 Mg ha^{-1}; above this point, biomass obviously increases. However, at average annual temperatures above 21°C, biomass does not vary with temperature.

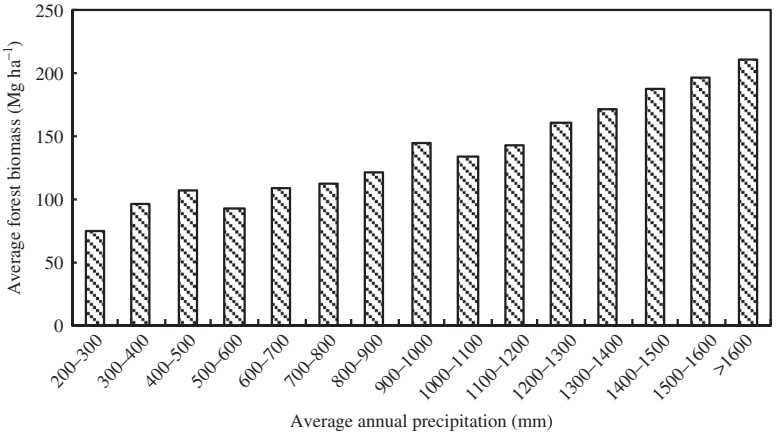

Figure 5. Allocation of forest biomass across the precipitation gradient within the NSTEC.

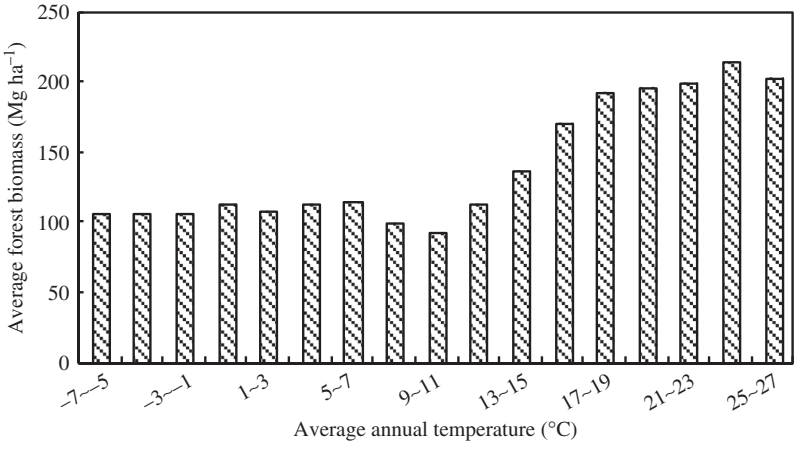

Figure 6. Allocation of forest biomass across the temperature gradient within the NSTEC.

According to the division of heat zones of China, an annual accumulated temperature of 4500°C represents the boundary between the warm temperate and subtropical zones. Because 12°C average annual temperature corresponds to 4500°C accumulated temperature, we can conclude that biomass significantly increases at the transition area from warm temperate to subtropical zones.

4. Conclusions

In this work, multiple linear regression models were developed to estimate the NSTEC regional forest biomass using a large body of field biomass, remote-sensing data, meteorological data, and topographic data. The results of statistical tests indicate that the estimates are reasonable and can truly reflect biomass distribution. Overall, forest biomass showed the same longitudinal trends between the southern and northern parts of the NSTEC (i.e. that biomass per unit forest area generally increases with increasing longitude). However, different latitudinal trends were found between the southern part of the NSTEC (dominated

by broadleaf forests) and the northern part (dominated by coniferous forests). In the northern part, the biomass per unit forest area showed relatively little fluctuation caused by the location of the Hinggan and Changbai Mountains. In the southern part, forest biomass was negatively correlated with latitude. Over the whole transect, high-intensity human disturbance and the development of secondary forest between 30° N and 40° N are important factors in the marked reduction in biomass. Therefore, there is a huge discrepancy in biomass at latitudes 37.5–40.0° N and 40.0–42.5° N. The average biomass density of coniferous forest was less than that of broadleaved forest. From the process and results of the modelling, we demonstrated that climate is the dominant factor affecting biomass. Both the quantity and distribution of air temperature and precipitation can directly affect biomass density.

Though the estimates we obtained are reasonable, errors still exist. Because it is difficult to obtain field-measured biomass data within the NSTEC, this article is mainly based on historical inventory data. These data were derived from various sources and ambiguous time ranges and cannot exactly match the TM data in time series, which may lead to estimation errors. The spatial mismatch between ground reference data and pixel size of the TM data is another likely source of error. The bands transition between MODIS and TM also reduced the precision of biomass estimation.

Acknowledgements

This research was supported by the National Natural Science Foundation of China (No. 40801138, No. 41071251), the National Key Basic Research and Development Programme (No. 2010CB833504), and the Non-Profit National Environmental Protection Industrial Special Research Project (No. 2011467030–01). The authors gratefully acknowledge Tianxiang Luo for his contribution to obtaining the biomass inventory data used in this study.

References

Barbosa, P. M., D. Stroppiana, J. M. Gregoire, and J. M. C. Pereira. 1999. "An Assessment of Vegetation Fire in Africa (1981–1991): Burned Areas, Burned Biomass, and Atmospheric Emissions." *Global Biogeochemical Cycles* 13: 933–950.

Curran, P. J., and A. M. Hay. 1986. "The Importance of Measurement Error for Certain Procedure in Remote Sensing of Optical Wavelengths." *Photogrammetric Engineering and Remote Sensing* 52: 229–241.

Dong, J. R., R. K. Kaufmann, R. B. Myneni, C. J. Tucker, P. E. Kauppi, J. Liski, W. Buermann, V. Alexeyev, and M. K. Hughes. 2003. "Remote Sensing Estimates of Boreal and Temperate Forest Woody Biomass: Carbon Pools, Sources, and Sinks." *Remote Sensing of Environment* 84: 393–410.

Foody, G. M. 2003. "Remote Sensing of Tropical Forest Environments: Towards the Monitoring of Environmental Resources for Sustainable Development." *International Journal of Remote Sensing* 24: 4035–4046.

Foody, G. M., D. S. Boyd, and M. E. J. Cutler. 2003. "Predictive Relations of Tropical Forest Biomass from Landsat TM Data and Their Transferability between Regions." *Remote Sensing of Environment* 85: 463–474.

Hame, T., A. Salli, K. Andersson, and A. Lohi. 1997. "A New Methodology for the Estimation of Biomass of Conifer-Dominated Boreal Forest Using NOAA AVHRR Data." *International Journal of Remote Sensing* 18: 3211–3243.

Hou, X. Y., ed. 2001. *Vegetation Atlas of China 1: 1 000 000*. Beijing: Science Press.

Huete, A. R. 1988. "A Soil-Adjusted Vegetation Index (Savi)." *Remote Sensing of Environment* 25: 295–309.

Hutchinson, M. F. 2001. *ANUSPLIN Version 4.2*. Canberra: Centre for Resource and Environmental Studies, Australian National University.

Lu, D. 2005. "Aboveground Biomass Estimation Using Landsat TM Data in the Brazilian Amazon." *International Journal of Remote Sensing* 26: 2509–2526.
Lu, D. 2006. "The Potential and Challenge of Remote Sensing-Based Biomass Estimation." *International Journal of Remote Sensing* 27: 1297–1328.
Luo, T. 1996. *Patterns of Net Primary Productivity for Chinese Major Forest Types and Their Mathematical Models*. Beijing: Commission for Comprehensive Survey of Natural Resources, Chinese Academy of Science.
Mayer, D. G., and D. G. Butler. 1993. "Statistical Validation." *Ecological Modelling* 68: 21–32.
Muukkonen, P., and J. Heiskanen. 2007. "Biomass Estimation Over a Large Area Based on Standwise Forest Inventory Data and ASTER and MODIS Satellite Data: A Possibility to Verify Carbon Inventories." *Remote Sensing of Environment* 107: 617–624.
Nelson, R. F., D. S. Kimes, W. A. Salas, and M. Routhier. 2000. "Secondary Forest Age and Tropical Forest Biomass Estimation Using Thematic Mapper Imagery." *Bioscience* 50: 419–431.
Peng, S. L., P. Zhao, H. Ren, and F. Y. Zheng. 2002. "The Possible Heat-Driven Pattern Variation of Zonal Vegetation and Agricultural Ecosystems Along the North-South Transect of China Under the Global Change." *Earth Science Frontiers* 9: 217–226.
Qi, J., A. Chehbouni, R. Huete, Y. H. Kerr, and S. Sorooshian. 1994. "A Modified Soil Adjusted Vegetation Index." *Remote Sensing of Environment* 48: 119–126.
Rossi, S., A. Rampini, S. Bocchi, and M. Boschetti. 2010. "Operational Monitoring of Daily Crop Water Requirements at the Regional Scale with Time Series of Satellite Data." *Journal of Irrigation and Drainage Engineering* 136: 225–231.
Roy, P., and S. A. Ravan. 1996. "Biomass Estimation Using Satellite Remote Sensing Data: An Investigation on Possible Approaches for Natural Forest." *Journal of Biosciences* 21: 535–561.
Thenkabail, P. S. 2004. "Inter-Sensor Relationships between IKONOS and Landsat-7 ETM+ NDVI Data in Three Ecoregions of Africa." *International Journal of Remote Sensing* 25: 389–408.
Tomppo, E., M. Nilsson, M. Rosengren, P. Aalto, and P. Kennedy. 2002. "Simultaneous Use of Landsat-TM and IRS-1c WiFS Data in Estimating Large Area Tree Stem Volume and Aboveground Biomass." *Remote Sensing of Environment* 82: 156–171.
Vermote, E. F., and A. Vermeulen. 1999. *Atmospheric Correction Algorithm: Spectral Reflectances (MOD09) – Version 4.0*. MODIS Algorithm Technical Background Document, Department of Geography, University of Maryland, p. 107.
Wu, S. H., Y. H. Yin, D. Zheng, and Q. Y. Yang. 2005. "Aridity/Humidity Status of Land Surface in China During the Last Three Decades." *Science in China Series D-Earth Sciences* 48: 1510–1518.
Wu, Z. 1980. *The Vegetation of China*. Beijing: Science Press.
Wylie, B. K., D. J. Meyer, L. L. Tieszen, and S. Mannel. 2002. "Satellite Mapping of Surface Biophysical Parameters at the Biome Scale Over the North American Grasslands: A Case Study." *Remote Sensing of Environment* 79: 266–278.
Zheng, D. L., J. Rademacher, J. Q. Chen, T. Crow, M. Bresee, J. Le Moine, and S. R. Ryu. 2004. "Estimating Aboveground Biomass Using Landsat 7 ETM + Data Across a Managed Landscape in Northern Wisconsin, USA." *Remote Sensing of Environment* 93: 402–411.
Zhou, G. S., and Y. J. Zhang. 2008. "Terrestrial Transect Study on Driving Mechanism of Vegetation Changes." *Science in China Series D-Earth Sciences* 51: 984–991.